

## Supramolecular Aggregation/Deaggregation in Amphiphilic Dipolar Schiff-Base Zinc(II) Complexes

Giuseppe Consiglio,<sup>†</sup> Salvatore Failla,<sup>\*†</sup> Paolo Finocchiaro,<sup>†</sup> Ivan Pietro Oliveri,<sup>‡</sup> Roberto Purrello,<sup>‡</sup> and Santo Di Bella<sup>\*‡</sup>

<sup>†</sup>Dipartimento di Metodologie Fisiche e Chimiche per l'Ingegneria, Università di Catania, I-95125 Catania, Italy, and <sup>‡</sup>Dipartimento di Scienze Chimiche, Università di Catania, I-95125 Catania, Italy

Received February 10, 2010

The synthesis, characterization, optical, and fluorescent properties of an amphiphilic Schiff-base bis(salicylal-diminato)zinc(II) complex are reported. Detailed <sup>1</sup>H nuclear magnetic resonance (NMR), diffusion-ordered spectroscopy (DOSY) NMR, optical absorption, and fluorescence spectroscopy studies indicate the existence of aggregate species in noncoordinating solvents. The degree and type of aggregation are related to the concentration and the polarity of the noncoordinating solvent. Dilute solutions are likely characterized by the presence of defined dimers, whereas larger oligomeric aggregates are conceivably formed at higher concentrations. The concentration needed to observe the formation of larger species depends upon solvent polarity. In coordinating solvents or in the presence of coordinating species, a complete deaggregation of the system occurs, because of the axial coordination to the Zn<sup>II</sup> ion, accompanied by considerable changes of <sup>1</sup>H NMR and optical absorption spectra. A dramatic enhancement of fluorescence emission is observed in dichloromethane solutions upon deaggregation with a coordinating agent. The formation of a defined 2:1 supramolecular structure is demonstrated in the case of a ditopic ligand as coordinating species. Overall, these complexes are promising systems for the development of new supramolecular architectures and supramolecular fluorescent probes.

### Introduction

Recently, there is a renewed interest in studying the diverse catalytic, optical, and photophysical properties associated with salen-based metal complexes.<sup>1</sup> Among them, Zn<sup>II</sup> complexes represent versatile synthons to supramolecular architectures.<sup>2</sup> Actually, their propensity toward the pentacoordination can lead to a variety of supramolecular assemblies.<sup>3,4</sup>

While aggregation via noncovalent bonds of strong dipolar chromophores, such as merocyanines, or extended  $\pi$ -conjugated species, such as perylene bisimide dyes or porphyrins, is governed by dipolar or  $\pi$ - $\pi$  stacking interactions, or a combination of them,<sup>5</sup> in tetracoordinated Zn<sup>II</sup> complexes, the driving force to aggregation occurs through the coordination to the metal center. As the pentacoordination can be achieved by the axial interaction of coordinating species or, in their absence, through intermolecular Zn $\cdots$ O axial coordination,<sup>2–4</sup> this allows for a different control of the supramolecular architecture. In this regard, it is attractive to explore such a phenomenon in solution, in the absence of coordinating agents, thus enabling aggregation, and eventually to investigate the deaggregation process upon addition of a coordinating species. Actually, the study of the aggregation in solution of these complexes is an almost unexplored field.<sup>4b</sup>

\*To whom correspondence should be addressed. E-mail: sfailla@dmfci.unict.it (S.F.) and sdbella@unict.it (S.D.B.).

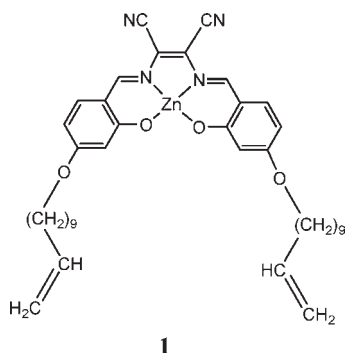
(1) For recent reviews see, for example: (a) Kleij, A. W. *Eur. J. Inorg. Chem.* **2009**, 193–205. (b) Kleij, A. W. *Chem.—Eur. J.* **2008**, *14*, 10520–10529. (c) Wezenberg, S. J.; Kleij, A. W. *Angew. Chem., Int. Ed.* **2008**, *47*, 2354–2364. (d) Clever, G. H.; Carell, T. *Angew. Chem., Int. Ed.* **2007**, *46*, 250–253. (e) Cozzi, P. G. *Chem. Soc. Rev.* **2004**, *33*, 410–421. (f) Di Bella, S. *Chem. Soc. Rev.* **2001**, *30*, 355–366. (g) Lacroix, P. G. *Eur. J. Inorg. Chem.* **2001**, 339–348.

(2) Kleij, A. W. *Dalton Trans.* **2009**, 4635–4639.  
(3) (a) Gallant, A. J.; Chong, J. H.; MacLachlan, M. J. *Inorg. Chem.* **2006**, *45*, 5248–5250. (b) Escudero-Adán, E. C.; Benet-Buchholz, J.; Kleij, A. W. *Inorg. Chem.* **2008**, *47*, 4256–4263. (c) Kleij, A. W.; Kuil, M.; Lutz, M.; Tooke, D. M.; Spek, A. L.; Kamer, P. C. K.; van Leeuwen, P. W. N. M.; Reek, J. N. H. *Inorg. Chim. Acta* **2006**, *359*, 1807–1814. (d) Kleij, A. W.; Kuil, M.; Tooke, D. M.; Lutz, M.; Spek, A. L.; Reek, J. N. H. *Chem.—Eur. J.* **2005**, *11*, 4743–4750. (e) Matalobos, J. S.; García-Deibe, A. M.; Fondo, D. N.; Bermejo, M. R. *Inorg. Chem. Commun.* **2004**, *7*, 311–314. (f) Reglinski, J.; Morris, S.; Stevenson, D. E. *Polyhedron* **2002**, *21*, 2175–2182.

(4) (a) Hui, J. K. -H.; Yu, Z.; MacLachlan, M. J. *Angew. Chem., Int. Ed.* **2007**, *46*, 7980–7983. (b) Ma, C. T. L.; MacLachlan, M. J. *Angew. Chem., Int. Ed.* **2005**, *44*, 4178–4182.

(5) For recent selected contributions of studies in solution see, for example: (a) Chen, Z.; Lohr, A.; Saha-Möller, C. R.; Würthner, F. *Chem. Soc. Rev.* **2009**, *38*, 564–584. (b) Lohr, A.; Grüne, M.; Würthner, F. *Chem.—Eur. J.* **2009**, *15*, 3691–3705. (c) Rösch, U.; Yao, S.; Wortmann, R.; Würthner, F. *Angew. Chem., Int. Ed.* **2006**, *45*, 7026–7030. (d) Würthner, F. *Chem. Commun.* **2004**, 1564–1579. (e) Würthner, F.; Yao, S.; Beginn, U. *Angew. Chem., Int. Ed.* **2003**, *42*, 3247–3250. (f) Würthner, F.; Yao, S.; Debaerdemaeker, T.; Wortmann, R. *J. Am. Chem. Soc.* **2002**, *124*, 9431–9447.

Chart 1



Schiff-base Zn<sup>II</sup> complexes have recently been investigated for their variegated fluorescent features, related to the structure of the salen template<sup>6</sup> and the axial coordination.<sup>7,8</sup> It is, therefore, of interest to investigate the factors determining aggregation of these complexes in solution, their photophysical properties in relation to the nature of the aggregate and upon deaggregation, and in the perspective of fluorescent supramolecular architectures.

The achievement of Zn<sup>II</sup> molecular species, sufficiently soluble in noncoordinating solvents, is therefore a prerequisite to investigate their aggregation in solution. To this end, we have obtained soluble Schiff-base Zn<sup>II</sup> complexes, even in low-polar noncoordinating solvents, by the achievement of amphiphilic species, and studied their aggregation in solution.

In this paper we report a detailed investigation on the structure and photophysical properties of aggregate amphiphilic dipolar Schiff-base Zn<sup>II</sup> complexes in solutions of noncoordinating solvents and their interesting optical changes upon deaggregation.<sup>9</sup>

## Results

The synthesis of the dipodal alkyl-derivatized complex **1** (Chart 1) was accomplished in a three-step approach involving a nucleophilic substitution reaction (the Williamson ether synthesis procedure) between 2,4-dihydroxybenzaldehyde and 11-bromo-1-undecene to form the 2-hydroxy-4-(undec-10-enyloxy)benzaldehyde derivative, followed by a condensation reaction with 1,2-diamine and, finally, complexation with

the Zn<sup>II</sup> cation.<sup>9</sup> The complex **1** is moderately soluble in low-polarity solvents, such as dichloromethane (DCM) and tetrachloroethane (TCE), and in some coordinating solvents, such as dimethyl sulfoxide (DMSO) and tetrahydrofuran (THF), and low-soluble in nonpolar solvents, e.g., toluene (TOL) and mesitylene (MES). Matrix-assisted laser desorption ionization-time-of-flight (MALDI-TOF) mass spectrometry analysis indicates the presence of defined signals corresponding to the protonated dimer, in addition to the protonated molecular ion (Supporting Information, Figure S1).

**<sup>1</sup>H NMR Studies.** <sup>1</sup>H NMR spectra of **1** in solutions of coordinating solvents, such as DMSO-*d*<sub>6</sub> or THF-*d*<sub>8</sub>, recorded at the concentration of  $\approx 4 \times 10^{-4}$  M, indicate the presence of sharp signals with the expected multiplicity, according to its molecular structure and consistent with the existence of monomeric species (Figure 1). As expected, these <sup>1</sup>H NMR spectra are independent from the concentration of the solution.

On switching to noncoordinating solvents, such as DCM-*d*<sub>2</sub> and TCE-*d*<sub>2</sub>, <sup>1</sup>H NMR spectra of **1**, recorded at the same above concentration, show a slightly broadening of the H<sub>3</sub> and H<sub>5</sub> peaks and a significant upfield shift (with respect to coordinating solvents) of the H<sub>1</sub> (0.15–0.35 ppm), H<sub>3</sub> (up to 0.65 ppm), and OCH<sub>2</sub>– (0.26–0.40 ppm) signals (Figure 1). These relevant upfield shifts, indicating that the involved hydrogens lie under the shielding zone of the  $\pi$  electrons of a conjugated system,<sup>5b,10</sup> and the observed peak broadening are both consistent with the existence of aggregate species of **1** in noncoordinating solvents.

<sup>1</sup>H NMR signals of **1** in noncoordinating solvents are concentration dependent. In particular, in the case of TCE-*d*<sub>2</sub> solutions with concentrations higher than  $1 \times 10^{-3}$  M, a progressive peak broadening of all aromatic hydrogens signals is observed, including those related to the OCH<sub>2</sub>– and CH=N groups, the latter of which is also upfield shifted, along with less shielding of H<sub>3</sub> aromatic protons (Figure 2). On the other hand, on going to lower concentrations,  $\leq 1 \times 10^{-3}$  M, <sup>1</sup>H NMR spectra are independent from the concentration. A similar behavior is observed in the case of DCM-*d*<sub>2</sub> solutions (Supporting Information, Figure S2). In fact, for concentrations higher than  $4 \times 10^{-4}$  M, the above-mentioned <sup>1</sup>H NMR signals become concentration dependent. Thus, <sup>1</sup>H NMR spectra recorded in almost saturated solutions of these noncoordinating solvents ( $\approx 2 \times 10^{-3}$  M in DCM-*d*<sub>2</sub> and  $\approx 1 \times 10^{-2}$  M in TCE-*d*<sub>2</sub>) are virtually identical, consisting of very broad signals involving all protons, with the exception of those related to alkyl chains, and this is typical of the presence of large aggregate species.<sup>4b</sup>

DOSY<sup>11</sup> has been used as an independent method to estimate the degree of aggregation and the molecular mass of **1**, through the measurement of the diffusion coefficient, *D*. This technique plays an important role in the identification of supramolecular species in solution owing to the straightforward two-dimensional (2D) representation of the components of the system. Equilibria between the aggregates are usually established in

(6) (a) Kuo, K.-L.; Huang, C.-C.; Lin, Y.-C. *Dalton Trans.* **2008**, 3889–3898. (b) Son, H.-J.; Han, W.-S.; Chun, J.-Y.; Kang, B.-K.; Kwon, S.-N.; Ko, J.; Han, S. J.; Lee, C.; Kim, S. J.; Kang, S. O. *Inorg. Chem.* **2008**, *47*, 5666–5676. (c) Lin, H.-C.; Huang, C.-C.; Shi, C.-H.; Liao, Y.-H.; Chen, C.-C.; Lin, Y.-C.; Liu, Y.-H. *Dalton Trans.* **2007**, 781–791. (d) Di Bella, S.; Leonardi, N.; Consiglio, G.; Sortino, S.; Fragalà, I. *Eur. J. Inorg. Chem.* **2004**, 4561–4565. (e) Ma, C.; Lo, A.; Abdolmaleki, A.; MacLachlan, M. J. *Org. Lett.* **2004**, *6*, 3841–3844. (f) Chang, K.-Hsien; Huang, C.-C.; Liu, Y.-H.; Hu, Y.-H.; Chou, P.-T.; Lin, Y.-C. *Dalton Trans.* **2004**, 1731–1738. (g) La Deda, M.; Ghedini, M.; Aiello, I.; Grisolia, A. *Chem. Lett.* **2004**, *33*, 1060–1061. (h) Wang, P.; Hong, Z.; Xie, Z.; Tong, S.; Wong, O.; Lee, C.-C.; Wong, N.; Hung, L.; Lee, S. *Chem. Commun.* **2003**, 1664–1665.

(7) (a) Cano, M.; Rodríguez, L.; Lima, J. C.; Pina, F.; Dalla Cort, A.; Pasquini, C.; Schiaffino, L. *Inorg. Chem.* **2009**, *48*, 6229–6235. (b) Germain, M. E.; Knapp, M. J. *J. Am. Chem. Soc.* **2008**, *130*, 5422–5423. (c) Germain, M. E.; Vargo, T. R.; Khalifah, G. P.; Knapp, M. J. *Inorg. Chem.* **2007**, *46*, 4422–4429. (d) Dalla Cort, A.; Mandolini, L.; Pasquini, C.; Rissanen, K.; Russo, L.; Schiaffino, L. *New J. Chem.* **2007**, *31*, 1633–1638.

(8) (a) Di Bella, S.; Consiglio, G.; Sortino, S.; Giancane, G.; Valli, L. *Eur. J. Inorg. Chem.* **2008**, 5228–5234. (b) Di Bella, S.; Consiglio, G.; La Spina, G.; Oliva, C.; Cricenti, A. *J. Chem. Phys.* **2008**, *129*, 114704/1–114704/5.

(9) For a preliminary communication of some aspects of this work see: Consiglio, G.; Failla, S.; Oliveri, I. P.; Purrello, R.; Di Bella, S. *Dalton Trans.* **2009**, 10426–10428.

(10) See, for example: Branchi, B.; Ceroni, P.; Balzani, V.; Cartagena, M. C.; Klärner, F.-G.; Schrader, T.; Vögtle, F. *New J. Chem.* **2009**, *33*, 397–407.

(11) (a) Morris, K. F.; Johnson, C. S., Jr. *J. Am. Chem. Soc.* **1992**, *114*, 3139–3141. (b) Johnson, C. S., Jr. *Prog. Nucl. Magn. Reson.* **1999**, *34*, 203–256.

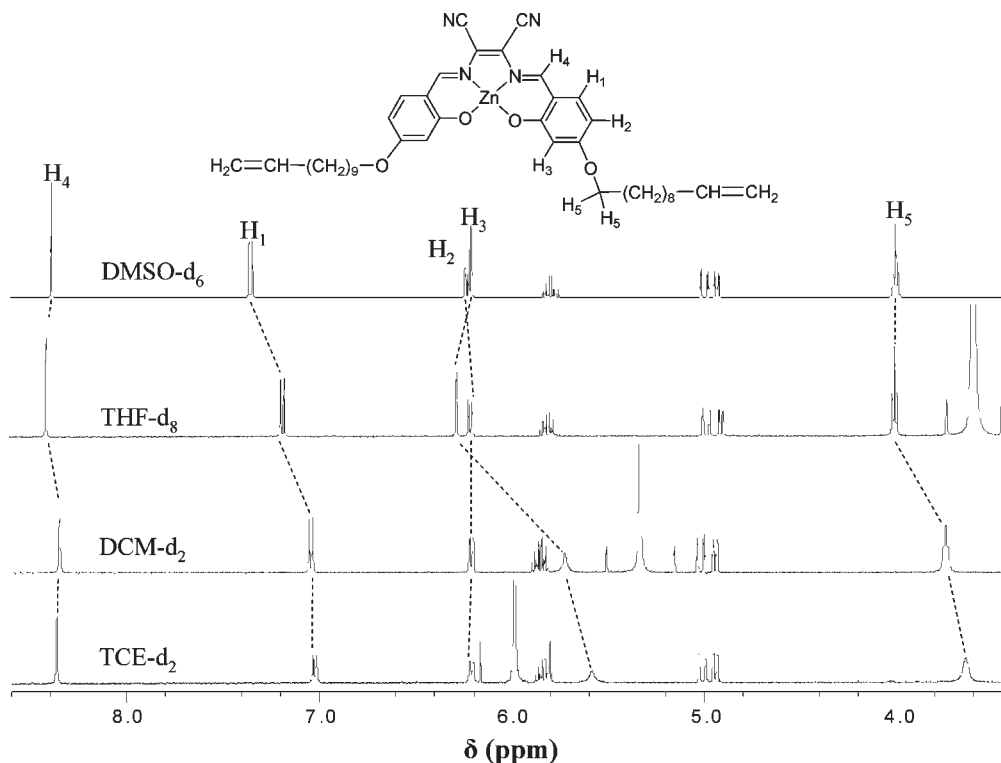


Figure 1.  $^1\text{H}$  NMR spectra of **1** ( $4.0 \times 10^{-4}$  M) in various solvents at  $27^\circ\text{C}$ .

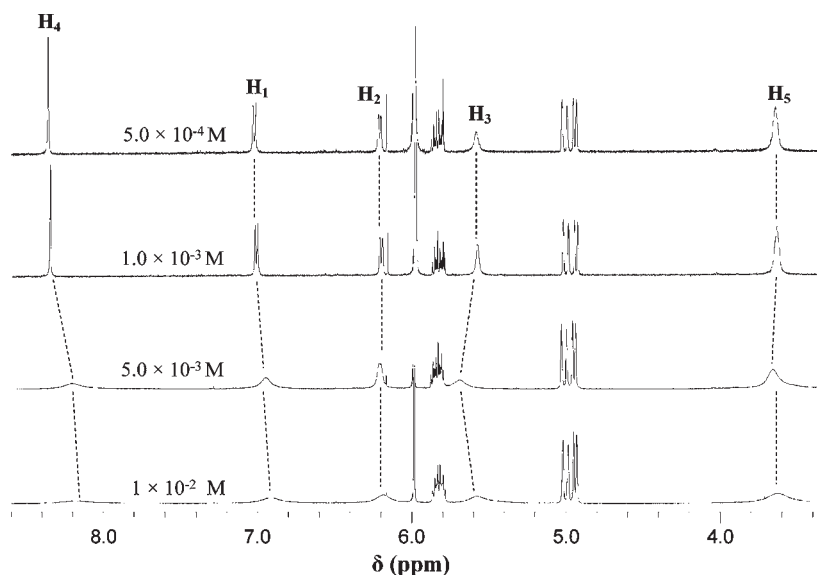


Figure 2. Concentration dependence of  $^1\text{H}$  NMR spectra of **1** in  $\text{TCE-}d_2$  solutions at  $27^\circ\text{C}$ .

solution and, if the interconversion rate is fast compared to the chemical shift NMR time-scale, then a single set of resonances is observed. This implies that the average diffusion value obtained from diffusion NMR experiments contains information about the level of aggregation.<sup>12</sup>

2D DOSY data collected from different concentrations of **1** in coordinating ( $\text{DMSO-}d_6$ ) and noncoordinating ( $\text{TCE-}d_2$ ) solvents are reported in Table 1 and are used to investigate the degree of aggregation of **1**, through an estimate of the molecular mass (see the Supporting Information for further details). They clearly indicate that the estimated molecular mass in  $\text{DMSO-}d_6$  is independent from the concentration of the solution, consistent with a monomeric  $\text{DMSO}$  axially coordinated species. In contrast, on switching to the  $\text{TCE-}d_2$  noncoordinating solvent, a concentration dependence of the diffusion coefficient is observed. In particular, while for

(12) (a) Macchioni, A.; Ciancaleoni, G.; Zuccaccia, C.; Zuccaccia, D. *Chem. Soc. Rev.* **2008**, *37*, 479–489 and references therein. (b) Pregosin, P. S. *Prog. Nucl. Magn. Reson. Spectrosc.* **2006**, *49*, 261–288. (c) Song, F.; Lancaster, S. J.; Cannon, R. D.; Schormann, M.; Humphrey, S. M.; Zuccaccia, C.; Macchioni, A.; Bochmann, M. *Organometallics* **2005**, *24*, 1315–1328.

concentrations  $\leq 1 \times 10^{-3}$  M the estimated molecular mass is independent upon dilution and consistent with a dimeric structure, for higher concentrations larger aggregates are predicted.

$^1\text{H}$  NMR studies of **1** in mixtures of noncoordinating/coordinating solvents (e.g., TCE- $d_2$ /DMSO- $d_6$  or DCM- $d_2$ /THF- $d_8$ ) further support the existence of aggregates in the former solvent. In fact, even in a mixture 1% v/v of the coordinating DMSO- $d_6$  (or THF- $d_8$ ) solvent are observed almost identical  $^1\text{H}$  NMR signals, in terms of peaks position and shape, as those recorded in pure DMSO- $d_6$  (or THF- $d_8$ ) solutions, indicating that the presence of coordinating species leads to a complete deaggregation of complex **1** in solution (see Supporting Information, Figures S3 and S4).

The deaggregation observed in solvent mixtures implies a large stoichiometric excess of the coordinating added species. Thus, it would be interesting to probe this effect with the addition of a stoichiometric amount of other coordinating species, such as pyridine. In fact, starting from a TCE- $d_2$  solution of **1**, the progressive addition of pyridine (see Supporting Information, Figure S5) results in a downfield shift and in a sharpening of  $\text{H}_1$ ,  $\text{H}_3$ , and the  $\text{OCH}_2-$  signals, which become almost identical to those observed in a THF- $d_8$  solution, upon addition of an equimolar amount of pyridine (Figure 3). Noteworthy, analysis of this  $^1\text{H}$  NMR spectrum (Figure 3) shows a substantial upfield shift and a broadening of the signal related to the *ortho*-hydrogen atoms of the pyridine.

**Table 1.** Diffusion Coefficients,  $D$ , and Estimated Molecular Mass,  $m$ , of **1** at 27 °C in Non-Coordinating (TCE- $d_2$ ) and Coordinating (DMSO- $d_6$ ) Solvents

concentration <sup>a</sup> ( $\times 10^{-3}$ M)	$D$ ( <b>1</b> ) ( $\times 10^{-10}$ m <sup>2</sup> s <sup>-1</sup> )	$D$ (solvent) ( $\times 10^{-10}$ m <sup>2</sup> s <sup>-1</sup> )	$m^b$ (Da)
5.0	2.37	8.05 (TCE- $d_2$ )	1948
1.0	2.88	8.30 (TCE- $d_2$ )	1402
1.0	3.55	8.01 (TCE- $d_2$ )	860 <sup>c</sup>
0.5	3.11	8.68 (TCE- $d_2$ )	1315
5.0	2.15	6.80 (DMSO- $d_6$ )	832
1.0	2.30	7.20 (DMSO- $d_6$ )	815

<sup>a</sup> The quasi-saturation regime of  $1 \times 10^{-2}$  M solutions of **1** in TCE- $d_2$  precluded the achievement of reliable DOSY data at these concentrations. <sup>b</sup> Estimated  $m$  with eq S4 in the Supporting Information. <sup>c</sup> Upon addition of a stoichiometric amount of pyridine.

This clearly indicates an axial coordination of pyridine to the complex. DOSY experiments further support these data. In fact, upon addition of a stoichiometric amount of pyridine to a  $1.0 \times 10^{-3}$  M solution of **1**, the increased diffusion coefficient and the estimated molecular mass are consistent with the formation of a monomeric, **1**·py species (Table 1). The addition of a stoichiometric excess of pyridine does not involve further changes in the  $^1\text{H}$  NMR spectrum as far as the peaks assigned to complex **1** are concerned (Supporting Information, Figure S5).

The effect of a coordinating ditopic ligand, such as the 1,2-bis(4-pyridyl)ethane (dpe), on the deaggregation of a TCE- $d_2$  solution of **1** was also investigated (Supporting Information, Figure S6). An analogous behavior, as that above observed upon addition of pyridine, can be verified. Actually, the  $^1\text{H}$  NMR spectrum obtained upon addition of a half molar amount of dpe is almost identical to that observed in a THF- $d_8$  solution (Supporting Information, Figure S7). Moreover, the *ortho*-hydrogen signals of dpe exhibit a substantial upfield shift and a broadening, indicating again an axial coordination of the ditopic dpe ligand to the complex.

**Optical Absorption and Fluorescence Spectroscopy Studies.** The UV-vis and emission spectra of **1** in a range of solvents of different polarities are shown in Figure 4, while relevant absorption and emission parameters are collected in Table 2. The absorption spectra in noncoordinating solvents consist of three main bands: an envelope between 300 and 400 nm, a band at  $\approx 430$  nm, and a feature between 500 and 540 nm. Moreover, on decreasing the solvent polarity, a progressive hypochromism of all bands is observed, accompanied by a marked change of the longer wavelength feature. In particular, the band centered at  $\approx 537$  nm in DCM splits in two defined peaks, whose new component appears to higher energy. These characteristics are consistent with the existence of various aggregate species. On switching to coordinating solvents (Figure 4), independently of their degree of polarity (Supporting Information, Figure S8), a more resolved structure between 300 and 400 nm is observed, with the appearance of two defined peaks and with the formation of a new, more intense band at  $\approx 550$  nm, which can be referred to the evolution of the longer wavelength feature

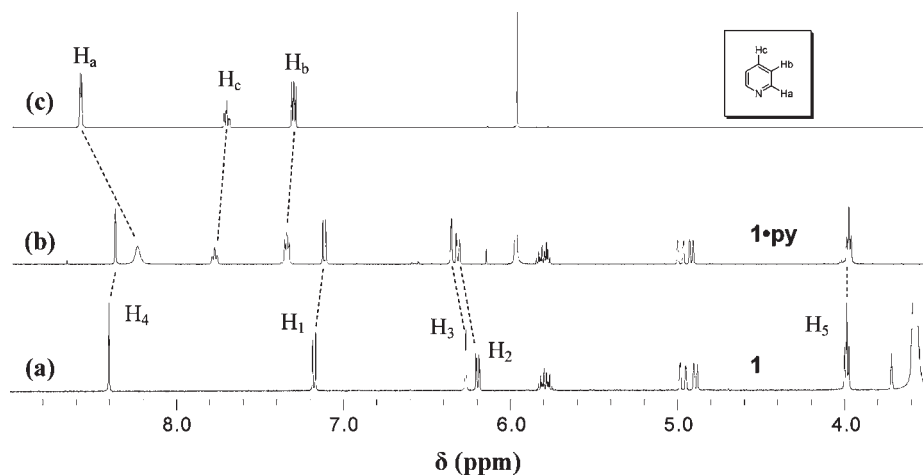


**Figure 3.**  $^1\text{H}$  NMR spectra of **1** in THF- $d_8$  (a) and **1**·py adduct in TCE- $d_2$  (obtained upon addition of an equimolar amount of pyridine to a TCE- $d_2$  solution of **1**) (b). The  $^1\text{H}$  NMR spectrum of pyridine in TCE- $d_2$  is reported for comparison (c).

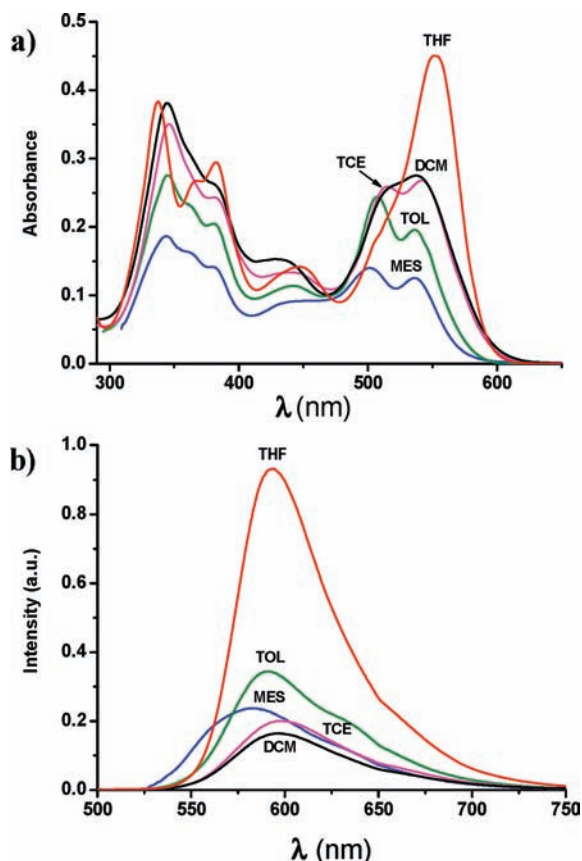


**Figure 4.** UV/vis absorption (a) and fluorescence (b) ( $\lambda_{\text{exc}} = 470$  nm) spectra of **1** ( $1.0 \times 10^{-5}$  M) in noncoordinating solvents of different polarities and THF.

**Table 2.** Absorption and Emission Parameters for Compound **1** in Various Solvents

solvent	absorption		emission	
	$\lambda_{\text{max}}$ (nm) <sup>a</sup>	$\epsilon$ (M <sup>-1</sup> cm <sup>-1</sup> )	$\lambda_{\text{max}}$ (nm) <sup>a,b</sup>	$\Phi$ <sup>c</sup>
MES	536	11 200	582	0.12
	501	12 600		
TOL	536	19 600	590	0.16
	507	24 400		
TCE	541	26 800	598	0.11
	515	25 900		
DCM	537	27 500	597	0.07
THF	551	45 000	593	0.24
ACN	542	36 500	599	0.07
py	562	45 000	615	0.18
DMSO	557	35 700	616	0.08

<sup>a</sup> Absorption and emission maxima are referred to  $1.0 \times 10^{-5}$  M solutions. <sup>b</sup>  $\lambda_{\text{exc}} = 461$  nm. <sup>c</sup> Fluorescence quantum yields were determined in  $2.5 \times 10^{-6}$  M solutions.

observed in noncoordinating solvents. These substantial changes are all indicative of monomeric species in solution upon axial coordination of the coordinating solvent to the Zn<sup>II</sup> metal center.

Steady-state fluorescence studies of **1**, in the same range of solvents, indicate the presence of an unstructured band with a maximum between 580 and 620 nm, independent from the excitation wavelength (Table 2 and Figure 4). In the case of noncoordinating solvents, emission features do not reflect the changes observed in optical absorption spectra (Supporting Information, Figure S9). Fluorescence

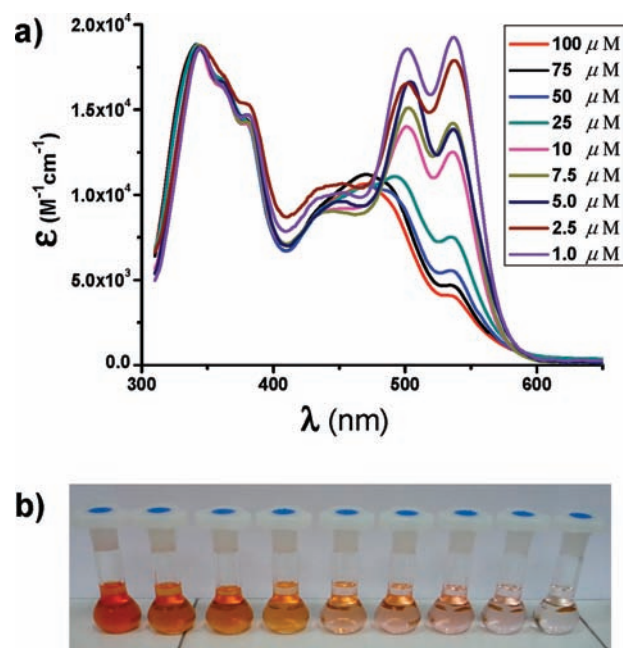


**Figure 5.** Concentration dependence (1.0–100  $\mu\text{M}$  range) of UV-vis absorption spectra of **1** in mesitylene solutions (a). Visual color changes (1.0–100  $\mu\text{M}$  range) from right to left (b).

quantum yields,  $\Phi$ , determined in a regime of low concentration, indicate variable, relatively low, values ( $\Phi = 0.08$ –0.16). Analogously, on going to coordinating solvents, the emission band maximum does not reflect the relative position of the lowest-energy band in the absorption spectra, and in the case of THF solutions, a sizable quantum yield value,  $\Phi = 0.24$ , is achieved.

Optical absorption spectra in noncoordinating solvents are strongly concentration dependent. For example, in the case of mesitylene solutions, a progressive, dramatic change of spectral features between 400 and 600 nm is observed in the range of concentration between  $1.0 \times 10^{-4}$  and  $1.0 \times 10^{-6}$  M (Figure 5). In particular, starting from dilute solutions and proceeding to higher concentrations, a continuous evolution of the two defined peaks at 501 and 536 nm can be observed, which coalesce in a structureless, blue-shifted feature. The most marked change occurs between  $1.0 \times 10^{-5}$  and  $2.5 \times 10^{-5}$  M, accompanied by a naked-eye observation of color change (Figure 5). An analogous concentration-dependence effect is observed in toluene solutions (Supporting Information, Figure S10). However, in low-polarity solvents, e.g., DCM, this effect is almost negligible, with a linear relationship of absorbance vs concentration plot. Some changes of optical absorption spectra can be observed just to higher concentrations  $\geq 5.0 \times 10^{-4}$  M, where the maximum of the lowest-energy band shifts to 518 nm (Supporting Information, Figure S11).

Related fluorescence response on varying the concentration of **1** in mesitylene solutions, in the above investigated range of concentrations, is rather variable in terms of  $\lambda_{\text{em}}$  maxima and related intensities and does not reflect the changes observed in optical absorption spectra (Figure 6). Fluorescence excitation spectra indicate an almost similar profile for all considered concentrations (Supporting Information, Figure S12), which can be essentially related to optical absorption spectra recorded

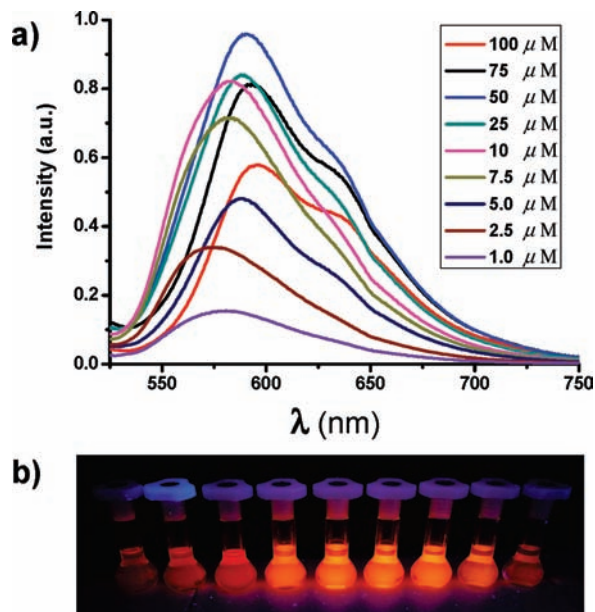


**Figure 6.** Concentration dependence (1.0–100  $\mu\text{M}$  range) of fluorescence spectra of **1** ( $\lambda_{\text{exc}} = 461 \text{ nm}$ ) in mesitylene solutions (a). Fluorescence of **1** (1.0–100  $\mu\text{M}$  range, from right to left) upon irradiation with a 366 nm UV lamp (b).

at lower concentrations ( $\leq 1.0 \times 10^{-5} \text{ M}$ ) (Supporting Information, Figure S12). In other words, even if absorption spectra indicate the existence of various aggregates of **1** in mesitylene, the emission can be mostly related to one species, while those observed in optical absorption spectra at higher concentrations seem to be less emissive. In fact, by increasing the concentration of the mesitylene solution results in a progressive attenuation of the fluorescence (Figure 6).

Deaggregation of **1** in solutions of noncoordinating solvents can be achieved by the addition of coordinating species. It involves dramatic changes in optical and fluorescence properties. For example, the addition of an equimolar amount of pyridine to a DCM solution of **1** leads to an optical absorption spectrum analogous to that observed in coordinating solvents, accompanied by a large enhancement of fluorescence, about one order of magnitude larger, in terms of integrated intensity (Figure 7). An analogous behavior is observed by adding DMSO, THF, or  $\text{CH}_3\text{CN}$  to a solution of **1** in DCM, even if the phenomenon occurs for a large stoichiometric excess of the coordinating added species (Supporting Information, Figure S13). In all cases, however, almost identical optical absorption spectra, fluorescence emission maxima and intensities, are achieved, presumably due to the complete deaggregation of complex **1** in solution upon axial coordination of the involved coordinating species to the  $\text{Zn}^{\text{II}}$  ion. A comparable effect is observed upon addition of a large stoichiometric excess of pyridine in mesitylene solutions of **1** (Figure 8), thus indicating an identical final state independent from the initial aggregate species. Moreover, the deaggregation process in mesitylene solutions ( $> 1.0 \times 10^{-5} \text{ M}$ ) involves an evident color change accompanied, however, by a less enhancement of fluorescence.

The effect of a coordinating ditopic ligand on the deaggregation of a DCM solution of **1** was also investigated. To this end, spectrophotometric and fluorimetric

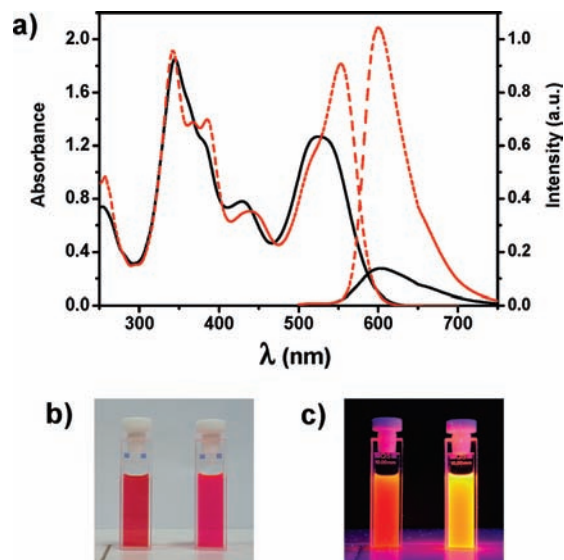


**Figure 7.** UV-vis absorption and fluorescence ( $\lambda_{\text{exc}} = 460 \text{ nm}$ ) spectra of **1** ( $5.0 \times 10^{-5} \text{ M}$ ) in DCM solutions (a) before (—) and after (---) the addition of an equimolar amount of pyridine. Visual color changes (b) and fluorescence (c) (upon irradiation with a 366 nm UV lamp) before (left) and after (right) the addition of an equimolar amount of pyridine.

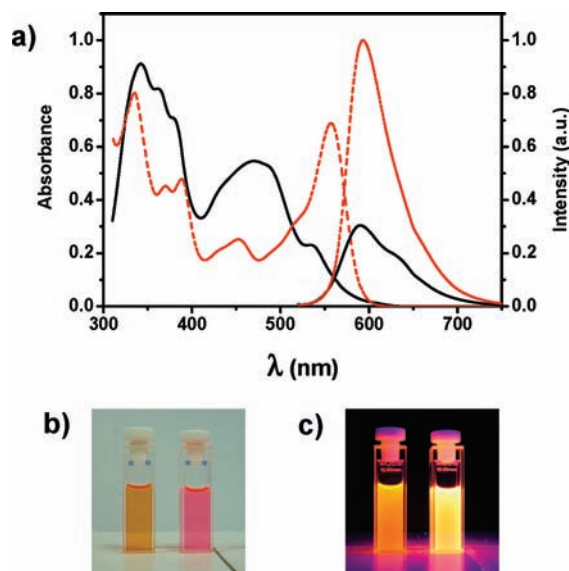


**Figure 8.** UV-vis absorption and fluorescence ( $\lambda_{\text{exc}} = 513 \text{ nm}$ ) spectra of **1** ( $5.0 \times 10^{-5} \text{ M}$ ) in mesitylene solutions (a) before (—) and after (---) the addition of a 10-fold mole excess of pyridine. Visual color changes (b) and fluorescence (c) (upon irradiation with a 366 nm UV lamp) before (left) and after (right) the addition of a 10-fold mole excess of pyridine.

titrations were performed using dpe as titrant (Figure 9). The changes of optical absorption spectra upon titration with dpe clearly indicate the formation of a defined single final species, as can be assessed by the presence of various isosbestic points. Moreover, a fluorescence enhancement is observed upon the addition of dpe. Interesting, both the absorption and fluorescence spectra at the end of the titration are identical to those observed upon addition of pyridine. This further confirms the same nature of the species in solution upon axial coordination. To determine the binding stoichiometry between the complex **1** and the

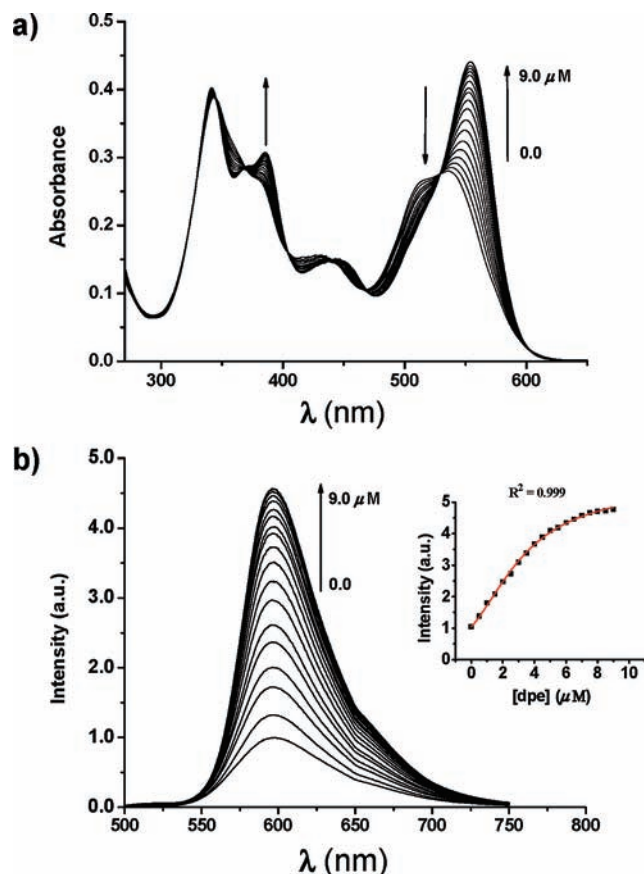


**Figure 9.** UV-vis absorption (a) and fluorescence (b) ( $\lambda_{\text{exc}} = 469$  nm) titration curves of **1** ( $10 \mu\text{M}$  solution in DCM) with addition of dpe. The concentration of dpe added varied from 0 to  $9.0 \mu\text{M}$ . Inset: variation of fluorescence intensity at 598 nm as a function of the concentration of dpe added. The solid line represents the curve fitting analysis with eq S1 in the Supporting Information.

dpe-coordinating species, the continuous variation method with fluorescence data was used.<sup>13</sup> Job's plot analysis (Figure 10) clearly indicates the formation of a supramolecular 2:1 structure, (**1**)<sub>2</sub>·dpe, (Supporting Information, Figure S14), according with the ditopic nature of dpe. Estimation of the binding constants from fluorescence titration data for a 2:1 binding model (see Supporting Information) indicates similar constants ( $\log K_1 = 5.1$  and  $\log K_2 = 5.4$ ).

## Discussion

The achievement of a simple dipolar Schiff-base Zn(II) complex having dipodal alkyl side chains in the salicylidene rings, relatively soluble even in low-polarity noncoordinating solvents, allowed us to perform a detailed study on its spectroscopic properties that, in turn, can be related to the aggregation/deaggregation process in solution.

<sup>1</sup>H NMR and DOSY studies indicate the existence of dimers of **1** in dilute solutions of noncoordinating solvents. In fact, the observed slightly broadening and upfield shift of some signals, on switching from coordinating to noncoordinating solvents, are in accord with definite aggregate species. The observed relevant upfield shift for H<sub>1</sub> and H<sub>3</sub> signals, which does not involve the H<sub>2</sub> and H<sub>4</sub> protons, indicates that these hydrogens lie under the shielding zone of the  $\pi$  electrons of a conjugated system. This view supports the formation of

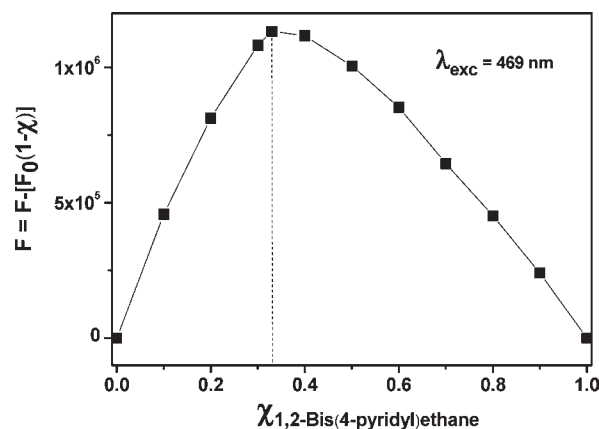
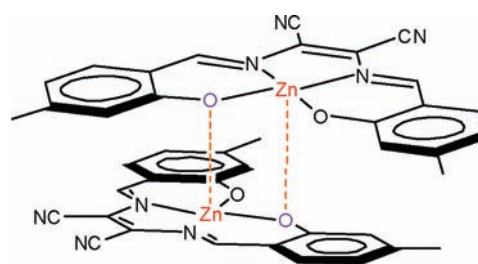


**Figure 10.** Job's plot for the binding of **1** with dpe in DCM. The total concentration of **1** and dpe is  $10 \mu\text{M}$ .

## Chart 2



defined dimer species in dilute solutions, e.g., in a staggered conformation,<sup>14</sup> in which both Zn atoms mutually interact through the  $\text{Zn} \cdots \text{O}$  axial coordination, thus fulfilling the coordination sphere of the  $\text{Zn}^{\text{II}}$  ion (Chart 2).

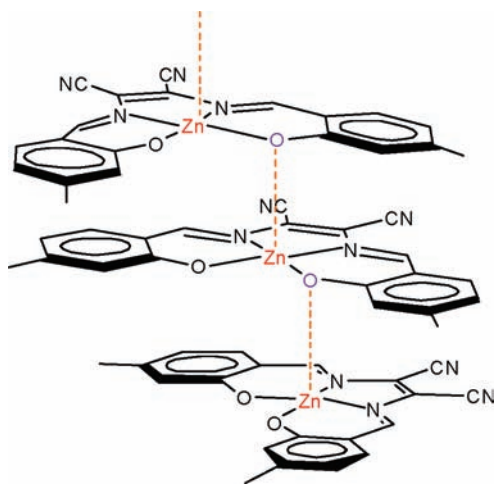
On going to higher concentrations, the observed decrease of diffusion coefficients, hence larger molecular masses, and the progressive and generalized peak broadening, involving all aromatic and imine <sup>1</sup>H NMR signals, indicate the existence of larger aggregates. In fact, the formation of oligomeric aggregates causes a broadening<sup>4b,15</sup> due to a significant decrease in the  $T_2$  relaxation time.<sup>16</sup> The different concentration threshold ( $> 4 \times 10^{-4}$  M for DCM and  $> 1 \times 10^{-3}$  M for TCE solutions) to observe formation of larger aggregates is dependent by the solvent polarity. This is consistent with the formation of larger oligomeric aggregates, involving an intermolecular  $\text{Zn} \cdots \text{O} \cdots \text{Zn}$  bridging coordination (Chart 3), presumably having an overall lower dipole moment than the dimers involved at lower concentrations, thus minimizing electrostatic interactions in concentrate solutions of low-polarity solvents. Moreover, the involvement of the nitrile

(14) Actually, selected 1D ROESY experiments of **1** in TCE-*d*<sub>2</sub> solutions ( $1.0 \times 10^{-3}$  M) indicate absence of intermolecular Overhauser effects (e.g., H<sub>3</sub>–H<sub>4</sub> through-space interactions), while only intramolecular Overhauser enhancements (e.g., H<sub>1</sub>–H<sub>4</sub>) are observed (Supporting Information, Figure S16). This implies the existence of aggregate structures in staggered conformations with the H<sub>3</sub> hydrogens lying over the CN groups of the adjacent units. This view is in agreement with the X-ray derived structures of some dimeric related Zn–salen complexes.<sup>3c,f</sup>

(15) See, for example: (a) Bilakhiya, A. K.; Tyagi, B.; Paul, P.; Natarajan, P. *Inorg. Chem.* **2002**, *41*, 3830–3842. (b) Tominaga, T. T.; Yushmanov, V. E.; Borisovitch, I. E.; Imasato, H.; Tabak, M. *J. Inorg. Biochem.* **1997**, *65*, 235–244.

(16) See, for example: (a) Sasaki, H.; Arai, H.; Cocco, M. J.; White, S. H. *Biophys. J.* **2009**, *96*, 2727–2733. (b) Da Costa, G.; Chevance, S.; Le Rumeur, E.; Bondon, A. *Biophys. J.* **2006**, *90*, L55–L57. (c) Evertsson, H.; Nilsson, S.; Welch, C. J.; Sundelöf, L.-O. *Langmuir* **1998**, *14*, 6403–6408.

Chart 3



groups in the formation of larger aggregates is ruled out because the CN-stretching frequency of **1** in DCM is unaffected by concentration.<sup>17</sup>

Optical absorption spectra also indicate the existence of aggregate species in noncoordinating solvents, as they are characterized by structureless features, with larger bandwidths and blue-shifted, compared to monomer ones in coordinating solvents. Moreover, they exhibit a marked concentration-dependence behavior that can be related to the solvent polarity. DCM solutions are characterized by the presence of a single species in a wide ( $1.0 \times 10^{-6}$ – $1.0 \times 10^{-4}$  M) range of concentration, according with the observed linear relationship of absorbance vs concentration (Supporting Information, Figure S11) and the <sup>1</sup>H NMR spectra recorded at low concentration ( $\leq 4.0 \times 10^{-4}$  M) (Supporting Information, Figure S2). The existence of defined species in dilute DCM solutions is corroborated by spectrophotometric titrations with dpe, which indicate the presence of multiple isobestic points. Conversely, in the same range of concentration of mesitylene or toluene solutions, both being almost nonpolar solvents, is observed a substantial change of optical absorption and fluorescence properties, consistent with the presence of different types of aggregates by varying the concentration. The absence of any isobestic point in the concentration-dependent optical absorption spectra (Figure 5 and Figure S10 in the Supporting Information) supports this hypothesis. In particular for dilute solutions

( $\leq 1.0 \times 10^{-5}$  M), optical absorption spectra and, hence, the nature of the aggregate species can be related to those observed in DCM or TCE solutions; the optical behavior at higher concentrations indicates the existence of different kinds of aggregates.<sup>18</sup>

On switching to coordinating solvents, <sup>1</sup>H NMR, DOSY, and optical spectroscopy data clearly indicate the presence of monomeric species of **1** in solution, because of the axial coordination of the solvent to the Zn<sup>II</sup> ion. Deaggregation of **1** in solutions of noncoordinating solvents, by addition of coordinating species, involves dramatic changes in optical and fluorescence properties. Thus, in the case of DCM solutions, the addition of an equimolar amount of pyridine leads to an optical spectrum analogous to that obtained in coordinating solvents and, more importantly, a remarkable enhancement of fluorescence. Deaggregation can be achieved with the addition of any coordinating species, even if it requires a variable stoichiometric amount of the latter. In any case, however, the system presumably reaches the same final electronic state, as almost identical optical absorption spectra, fluorescence emission maxima, and intensities are obtained. This is again owing to the complete deaggregation of complex **1** in solution upon axial coordination to the Zn<sup>II</sup> ion by the involved coordinating species. An analogous behavior is observed for mesitylene solutions of **1**, although in this case, the deaggregation process requires a large stoichiometric excess of pyridine. Actually, the deaggregation of **1** upon axial coordination to the Zn<sup>II</sup> ion necessarily involves formation of a polar species; hence, the deaggregation process becomes unfavorable in nonpolar solvents.

The use of a ditopic ligand as coordinating species offers the possibility to build new supramolecular architectures. Thus, the formation of a defined 2:1 supramolecular structure, (**1**)<sub>2</sub>·dpe, is demonstrated by <sup>1</sup>H NMR analysis and the existence of multiple isobestic points in optical absorption spectra upon spectrophotometric titrations (Figure 9) and is further confirmed by Job's plot analysis (Figure 10). As expected from the two independent binding sites of dpe to complex **1**, similar binding constants ( $\log K_1 = 5.1$  and  $\log K_2 = 5.4$ ) were estimated according to the intermediate value found for the **1**·py binding constant ( $\log K = 5.3$ ).<sup>9</sup>

## Conclusions

Amphiphilic dipolar Schiff-base Zn<sup>II</sup> complexes, relatively soluble in a wide variety of solvents, ranging from polar coordinating to nonpolar noncoordinating species allowed performing a detailed study on their spectroscopic properties, in relation to the aggregation/deaggregation process in solution.

While in noncoordinating solvents these complexes are always aggregates, but in coordinating solvents they are monomeric because of the axial coordination of the solvent to the Zn<sup>II</sup> metal center. The degree and type of aggregation are related to the polarity and the concentration of the noncoordinating solvent. Dilute solutions are likely characterized by the presence of defined dimer aggregates, whereas larger oligomeric aggregates are conceivably formed at higher concentrations. The threshold of concentration in which this is observed depends upon solvent polarity. The switching to the monomer can be driven by

(17) (a) FT-IR spectra of **1** in DCM solutions recorded at different concentrations ( $4.0 \times 10^{-4}$ ,  $1.0 \times 10^{-3}$  M) indicate an identical frequency ( $2220 \text{ cm}^{-1}$ ) as far as the CN-stretching mode is concerned.<sup>17b</sup> The band remains almost unchanged ( $2218 \text{ cm}^{-1}$ ), even with the addition of a stoichiometric excess of pyridine. This indicates that the CN groups are not involved in the aggregation/deaggregation processes of **1** in noncoordinating solvents. (b) Lacroix, P. G.; Di Bella, S.; Ledoux, I. *Chem. Mater.* **1996**, *8*, 541–545.

(18) (a) Unfortunately, the relatively low solubility of **1** ( $\leq 1.0 \times 10^{-4}$  M) in mesitylene or toluene solutions, together with a concomitant slightly demetalation<sup>18b</sup> under these conditions, precluded reliable <sup>1</sup>H NMR measurements in these deuterated solvents. To improve the solubility in nonpolar solvents, the synthesis of the related 4-(hexadecyloxy) derivative, **2**, was accomplished (see the Supporting Information for details). Compound **2**, possessing an almost identical, as to **1**, optical behavior on switching from noncoordinating to coordinating solvents (Supporting Information, Figure S17), is still insufficiently soluble in nonpolar solvents to achieve accurate <sup>1</sup>H NMR data. (b) Wezenberg, S. J.; Escudero-Adán, E. C.; Benet-Buchholz, J.; Kleij, A. W. *Org. Lett.* **2008**, *10*, 3311–3314.



the addition of a coordinating species and involves substantial optical variations and a dramatic enhancement of the fluorescence emission.

Overall, these characteristics are relevant in the perspective of new supramolecular architectures and in the development of supramolecular fluorescent probes.

**Acknowledgment.** This research was supported by the MIUR.

**Supporting Information Available:** Experimental section and additional  $^1\text{H}$  NMR, DOSY, and optical spectroscopic data, as noted in the text. This material is available free of charge via the Internet at <http://pubs.acs.org>.